Recent advances in the alignment of silicon mirrors for high-resolution x-ray optics

Kai-Wing Chan, James R. Mazzarella, Timo T. Saha, William W. Zhang, Michael P. Biskach, et al.

Kai-Wing Chan, James R. Mazzarella, Timo T. Saha, William W. Zhang, Michael P. Biskach, Ai Numata, Raul E. Riveros, Ryan S. McClelland, Peter M. Solly, "Recent advances in the alignment of silicon mirrors for high-resolution x-ray optics," Proc. SPIE 11119, Optics for EUV, X-Ray, and Gamma-Ray Astronomy IX, 111190A (9 September 2019); doi: 10.1117/12.2528746

SPIE.

Event: SPIE Optical Engineering + Applications, 2019, San Diego, California, United States

Recent Advances in the Alignment and Bonding of Silicon Mirrors for High-Resolution Astronomical X-ray Optics

Kai-Wing Chan[1,a,c], James R. Mazzarella[b,c], Timo T. Saha[c], William W. Zhang[c], Michael P. Biskach[b,c], Ai Numata[b,c], Raul E. Riveros[a,c], Ryan S. McClelland[a], Peter M. Solly[b,c]

[a]Center for Research and Exploration in Space Science and Technology & University of Maryland, Baltimore County, Baltimore, MD 21250
[b]KBR Inc., Spacer Engineering Division, 7701 Greenbelt Road, Greenbelt, MD 20770
[c]NASA/Goddard Space Flight Center, Greenbelt, MD 20771

ABSTRACT

Recent advances in the fabrication of segmented silicon mirrors make it possible to build large-area, lightweight, high-resolution x-ray telescopes with arc-second angular resolution. To build such a telescope, we fabricate accurate silicon mirrors and develop alignment and bonding techniques to precisely align and integrate these silicon mirror segments into modular units. In this way, the processes of mirror fabrication, mirror alignment and bonding, and subsequent integration into units of successive larger scale are completely independent, and their technologies can be developed independently. In this paper, we present recent improvement in the precision of optical alignment and mirror bonding. We discuss the measurement of the mirror's focusing in a parallel optical beam and address the practical challenges in bonding these mirrors into modules as an intermediate step to build up a full-scale telescope for space missions.

Keywords: X-ray optics, lightweight mirrors, segmented mirrors, silicon mirrors, mirror alignment, mirror bonding

1. INTRODUCTION

The next ambitious x-ray missions for astronomy, such as *Lynx*[1,2], demand a telescope having a large effective area, good angular resolution, and broadband response. To achieve a large effective area in a grazing-incidence x-ray telescope, lightweight reflectors capable of supporting a telescope with high area-to-mass ratio as large as 10 cm^2/kg in the soft x-ray band are required. To this end, integrating segmented mirrors into modules and assembling the modules into a successively larger unit is currently the only practical approach to achieve a large, 1-2 m^2 effective area class telescope.

In this hierarchical approach, a high-resolution x-ray telescope begins with precisely integrating high-resolution mirror segments into modules. At NASA/Goddard Space Flight Center (GSFC), we adopt the principle that first requires fabrication of the most accurate mirror segments, and subsequent mirror alignment that is distortion-free[3]. That is, there is no assumption, during the process of alignment and integration, on the provision of correction of any imperfection in mirror figure. With such an approach, the technologies of mirror fabrication, mirror alignment and bonding, and integration of modules can be independently developed, and the implementation of various processes to build the telescope need not be substantially linked together.

As previously reported[4], our x-ray mirror group at GSFC uses mono-crystalline silicon as our mirror substrates. The primary advantage of using crystalline silicon is that it is practically free of internal stress. This quality allows polishing precise mirrors without introducing additional stress that will distort the mirror. Any surface damage/stress can be removed with adequate etching. In addition, the high thermal conductivity and low coefficient of thermal expansion of silicon also provides the needed thermal uniformity for a high-resolution telescope. These mirrors are

[1] Kai-Wing.Chan-1@nasa.gov

Optics for EUV, X-Ray, and Gamma-Ray Astronomy IX, edited by Stephen L. O'Dell, Giovanni Pareschi, Proc. of SPIE Vol. 11119, 111190A · © 2019 SPIE · CCC code: 0277-786X/19/$21 · doi: 10.1117/12.2528746

then aligned and integrated, in successively larger scales, into a space telescope[4]. The technology steps of building up a high-resolution telescope are therefore: (1) Fabrication of precise mirrors, which includes manufacturing precise substrates and stress-free polishing[5]; (2) Distortion-free metallic coating on the surface of the substrate to enhance its x-ray reflectivity[6,7,8,9]; (3) Precise alignment of mirrors[10]; (4) Bonding of mirrors, in our case, using epoxy, into a modular structure without introducing additional unacceptable distortion[10]; (5) Building up a module; (6) Alignment and integration of modules into a telescope[11,12].

Here we note that we research and develop every one of these technological steps. We report recent development of them in these conference proceedings. The general concept and current status of building a large, high-resolution astronomical x-ray telescope, is reviewed[13] in a paper by Zhang, et al. (for a discussion in the specific context of the Lynx mission concept, see Zhang et al.[3]) Critical technologies are discussed in separate papers. The fabrication of accurate silicon mirrors is reported in a paper by Riveros, et al.[14]. Issues with metallic coating and promising techniques to eliminate/balance the coating stress are addressed in Yao et al.[15], and Zuo et al.[16] This present paper reports on the alignment and bonding of mirrors, and on their precision and stability[17]. Integration of mirrors into modules, with emphasis on key issues in module production and production efficiencies, are discussed in Biskach et al.[18] The paper by Solly et al.[19] addresses in details the structural and thermal analyses of a generic telescope. Finally, options for various optical designs of large x-ray telescopes are addressed in a paper by Saha et al.[20]

2. ALIGNMENT OF MIRRORS

Given an accurate silicon mirror, the task of alignment is to position it precisely and efficiently so that grazing incidence will produce sharp, sub-arcsecond focus in x-rays. Since it is inefficient to align and bond mirrors in x-ray wavelength, which requires a vacuum environment, we carry out mirror alignment in optical wavelength under atmospheric condition. The current setup is shown in Figure 1.

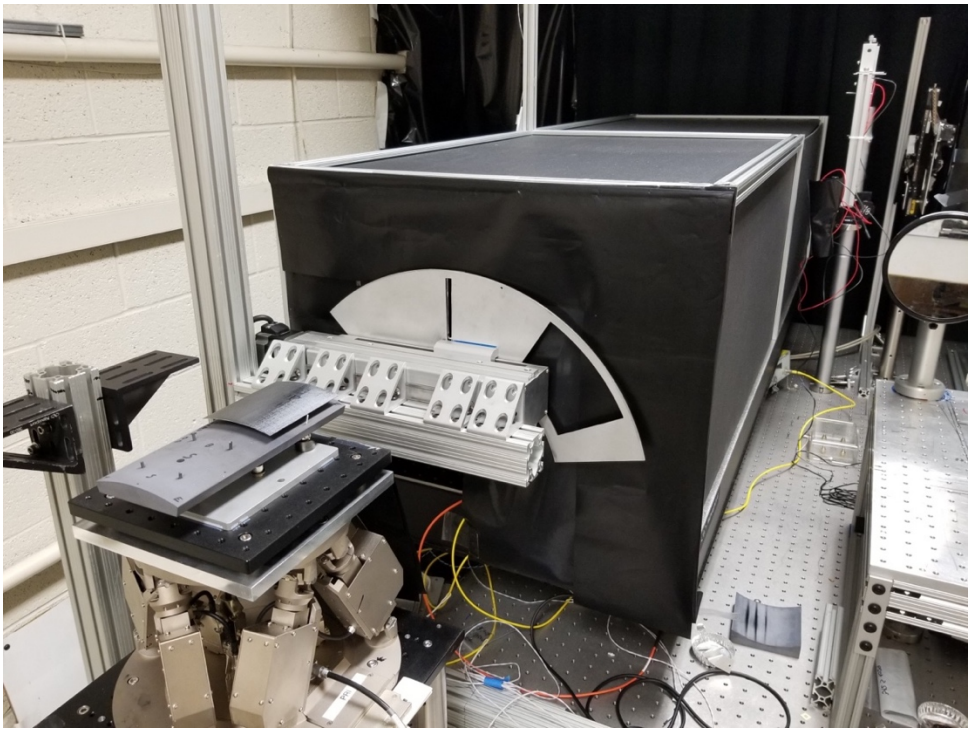

Figure 1. The alignment setup consists of a light source, a movable mask, a platform with adjustable tip/tilt, a set of folding mirrors and a CCD detector (not shown). A parallel beam is generated with an off-axis paraboloidal mirror of 300 mm diameter from a laser point source of 5 μm. The image, after grazing-incidence reflection from the silicon mirrors to be aligned, is focused on the detector.

The mirror to be aligned is placed in a parallel optical beam so that a focused image is generated at the focal plane. Highly diffracted images are collected at the charge-coupled device (CCD). A movable slit sub-divides the incident beam in the azimuthal direction. The distribution of the centroids of these images determine the goodness of the focusing.

A few words on the dimensions of our typical test articles are listed as follows. The focus of the system under investigation is 8400 mm, with mirror radius in the range of 155–160 mm. 30-degree segments are chosen, giving an azimuthal (arc) length of mirrors of 81–84 mm. The axial length of the mirror is 100 mm. The mirror system is a two-reflection (Wolter I) system. The incidence angle of the primary mirror is about 0.26°–0.27°, while that of the secondary mirror is about 3 times larger. For these cylinder-like segments, we use a 4-point mounting scheme in which 4 posts, which are actually spacers between the mirrors in consecutive shells (in the following, when the context is clear, we use the terms "post" and "spacer" interchangeably), are arranged in a rectangular grid. In the azimuthal direction, the separation of the posts is 15° in angular span; the separation of the posts in the axial direction is 56 mm. The posts themselves have a diameter ranging from 1 mm to 4.25 mm.

To carry out the alignment, a mirror is first placed on the four posts. It is then shaken, either acoustically or mechanically, to settle it into place. Sub-aperture images are then taken to determine the goodness of the focus, which, in turn, determines the correction of the post heights required. The mirror is then removed from its mount and the mount is taken to have its post heights corrected. The process is refined once or twice to refine the mirror focusing. In the following, we discuss the critical technological issues of these steps.

2.1 Placement of mirror segments

Each mirror is simply-supported by four spacers. Due to the cylindrically rotational symmetry of the mirror segment (which is roughly a segment of a conical surface) and its approximate translational invariance in the axial direction (the underlying cone has a small cone angle), the mirror supported in this way is practically statically determined. The four supporting points do not over-constrain the mirror. Depending on the diameter of the spacers, they do obscure the aperture slightly (2.5% for 1 mm spacers.)

It is noted that the surface of a mirror is that of a revolution generated from a parabola or hyperbola, which has a perfect rotational symmetry. Of the remaining 5 degrees of freedom (DoF), the translation along the axis is approximately invariant, due to the small angle of incidence. For the test mirrors with the aforementioned dimensions, the sensitivity is only about ¼ seconds of arc at the 8400 mm focal length for every 1 mm axial displacement. Since we can easily place the mirror with 1 mm precision, we take advantage of this insensitivity to axial translation and consider this axial translation also invariant. The remaining 4 DoF of the mirror supported by the 4 spacers are uniquely determined by the height of the spacers. The 4 DoF to be determined are: X and Y translations in a plane parallel to the focal plane, and the rotations of the mirror corresponding to the yaw angle (rotation about the radial direction) and pitch angle (rotation about an axis in the general azimuthal direction) of the mirror (the remaining angle, the rotation about the optical axis, is the roll angle). In practice, additional axial and azimuthal stops hold the solid mirror so that it will not roll or slide away.

The scheme above works only if the mirror is in contact of each spacer at a single point at a specified location. A spacer with a flat top, for example, will contact the mirror at ambiguous and shifting locations. When that happens, the subsequent process of spacer-height correction will not converge. We therefore machine the spacer top so that it has a crown-shaped surface, which also provides an additional benefit in that the epoxy applied during mirror bonding can readily spread out to allow contact of the mirror to the spacers. We develop machining techniques to cut either conical-top or spherical-top spacers. However, in order to have sufficient space for the epoxy to spread out, the radius of the spherical-top spacer will be quite small (for example, to have ~ 70 μm clearance for a spacer with 2 mm diameter, the top of the spacer will have a radius of curvature of about 7 mm.) The same clearance can readily be accommodated with a conical top with a 4° inclination. For this reason, we mostly use conical-top spacers which work fine so far.

Without additional assistance, friction between the spacers and the mirror will prevent the mirror from settling onto its mathematically determined position. If not done properly, the mirror may be sitting on three of the four spacers only. To settle the mirror into place, a number of methods of agitation have been used: vibration of the base of the mount either by simple tapping, or by using a small vibrational motor, or by acoustic agitation. Sound waves

have the advantage of directly vibrating the topmost mirror, which is typically the mirror in question. The other mirrors are somewhat shielded and the supporting structure is relatively massive. Vibration on the mirror mount necessarily sends high frequency vibration through the spacers (or other existing intermediate mirrors). However, using acoustic wave can be an environmental hazard, especially when heavier mirrors are to be aligned, and ear protection is required for the operator and other lab personnel. We have been using both methods and are still developing methods that are safe and effective.

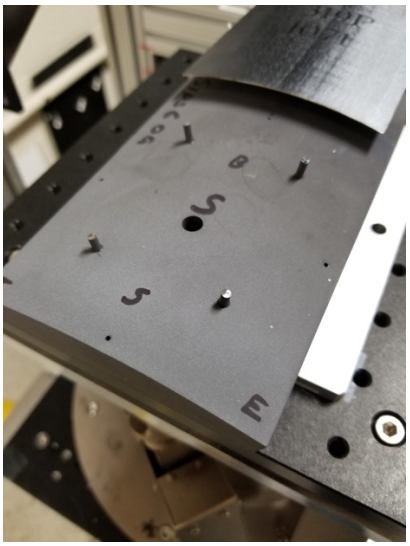

Figure 2. A mirror mount with 4 spacers. The test mount can accommodate two mirrors (for the primary and secondary mirrors in a 2-reflection system). The spacers shown are made of silicon and have cone-shaped top surfaces. The spacers' top surfaces are ground.

Another point that we should note is about distortion under gravity. Needless to say, these thin silicon mirrors are not perfect rigid bodies. There is a mild gravity distortion of the mirrors that will impact performance at the level of 1". To minimize the gravity distortion, we choose the spacer separations with the dimensions stated above.

2.2 Determination of image focusing by optical Hartmann measurements

The proper alignment of the mirror is determined by the focusing quality of the image it produces in the focal plane, which, in turn, is determined by the concentration of the centers of the azimuthal sub-aperture images. The sub-apertures come from slits placed between the mirror and the optical beam which is co-aligned with the overall optical axis of the system, as shown in Figure 1. Such sub-aperture Hartmann measurements produce highly diffracted images (largely in the radial direction due to the small angle of incidence). Roughly, from the distribution of the image centers, the span in the azimuthal direction gives a pitch angle error, while the span in the radial direction gives the yaw error. The displacement of the mirror in the plane parallel to the focal plane (the X and Y translation) is, in principle, determined by the distance of the overall image focus from point where the optical axis meets the focal plane. However, the position of the image focus is very insensitive to the X and Y displacement, (sensitivity ~ $6.48 \times 10^5/(\pi f)$ ″/μm ~ 0.024″/μm, for f = 8400 mm) and the mirror displacement can be much better determined by other means (more on this below). That is, the two angular error terms are the only significant error terms.

We use a diode laser source placed at the focus of a 300-mm off-axis parabolic mirror to generate the collimated beam. Each sub-aperture exposure produces a highly diffracted image in the radial direction. Even though the images are highly diffracted, their centroids are assumed to represent the actual image centers from reflection of x-rays. In fact, it has been shown that for an angle of incidence of ~ 0.5°, the precision is about 0.3″ when the image background is properly subtracted. This precision has been tested against x-ray results. Examples of the image profiles are shown in Figure 3. The size of the diffracted image, s, goes with the inverse of the angle of incidence: $s \sim \lambda/$(opening width) * $f \sim \lambda f / (a\ \alpha)$, where λ is the wavelength of the incident light, f is the focal length of the mirror, a is the length of the mirror, α is the angle of incidence. That is, there is a large difference between mirrors in the first (primary) stage

and that of the second (secondary) stage. In the generic Wolter-I design, the focal length of a primary mirror is about 3 times that of the secondary, while the angle of incidence is 3 times smaller. The size of the image from a primary mirror is nearly an order of magnitude larger than that of the secondary mirror on their focal planes (while the light captured is only 1/3). This causes a more serious diffraction issue for primary mirrors compared to secondary mirrors. The determination of centroids is worse due both to larger statistical and systematic errors. Currently, the repeatability of centroid determination for the secondary test mirrors with the aforementioned dimensions is about 0.3", while that for the primary mirrors is > 1″ and is dominated by systematic uncertainty such as stray light and spurious fringes. We are working to resolve those issues.

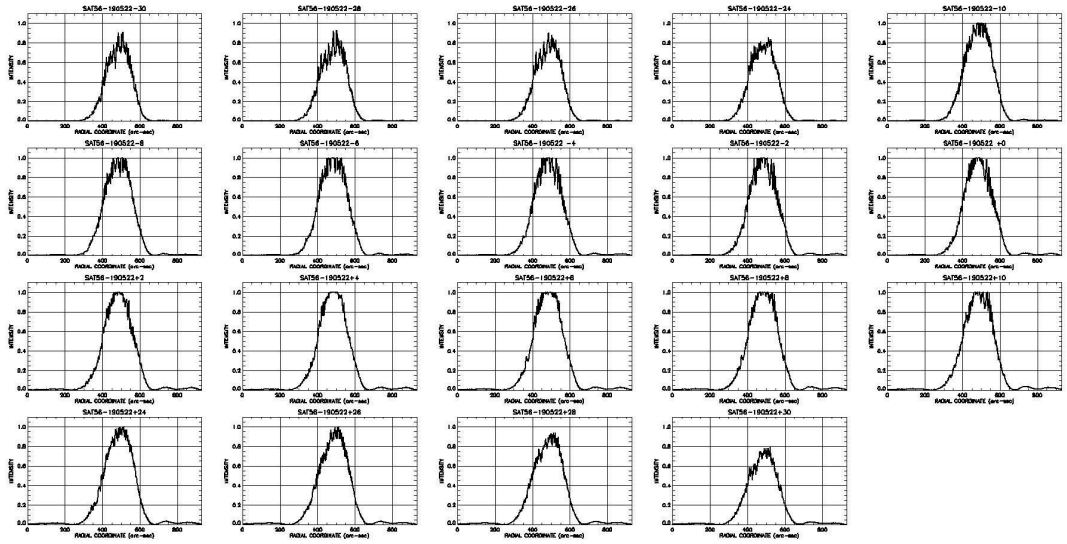

Figure 3. Example of light distribution of diffracted sub-aperture images. Deviation from perfect smoothness and secondary diffraction peaks can be seen. The centroids of the images represent the quality of the mirror alignment.

As mentioned before, the remaining two translational degrees of freedom for the mirror alignment cannot be precisely determined by the Hartmann measurements. Instead, they are determined separately by a set of radius probes (Figure 4). These probes measure the radius directly with a resolution of 0.1 μm. The actual repeatability is slightly worse, at approximately 0.2 μm, due to precision in placing the mirror mount repeatably, and to some extent temperature effect. The probes are mounted on a stiff stainless-steel structure. This is a potential issue with CTE-mismatch, if the temperature of the environment is not well controlled. For the setting of the translational degrees of freedom, a precision of a few μm is quite sufficient (for a typical sensitivity of 0.024″/μm). In fact, the spacers on the mirror mount were preset with the radius probes, so that, practically, the linear alignment errors are not dealt with and only the angular alignment errors are corrected. The amount of correction for the angular alignment errors are of the order of 1 μm and they do not practically affect the mirror translational displacement.

The insensitivity of alignment to linear displacement has an additional beneficial effect. In the actual process of spacer height adjustment, the spacer height can only be reduced. This fact limits the exact solution of spacer correction. The insensitivity allows a slight displacement (μm) of the mirror without affecting the alignment in practice. It should be noted that the fact that the spacer height cannot be increased will become a real constraint towards a true solution, when the alignment requirement is closer to 0.1″.

The absolute calibration of the probes, in principle, can be set with an accurate reference. As of now, we do not have such an absolute reference available. Instead, for the task of setting relative linear dimensions correctly, we use two commercial flats, one for each of the two sides of the mirrors, to set the spacer heights. Such reference determines the spacer heights to 0.2 μm, the repeatability of the probe measurements, subjected to an unknown overall tilt, which is unimportant as all angular terms are more accurately determined by the Hartmann measurements. The other drawback with using two flats is that the spacer heights on the two sides of the mirrors cannot be related to each

other. Such uncertainty results in an overall roll angle error, which, as we discuss before, is not relevant for a single pair of mirrors. We do have an absolute reference, however, using a mirror mount that has been built previously, and that has been demonstrated in prior x-ray test that its alignment is good (to 1″). This artifact serves as an absolute reference for all 8 points for now, until we can obtain a certifiably more accurate reference.

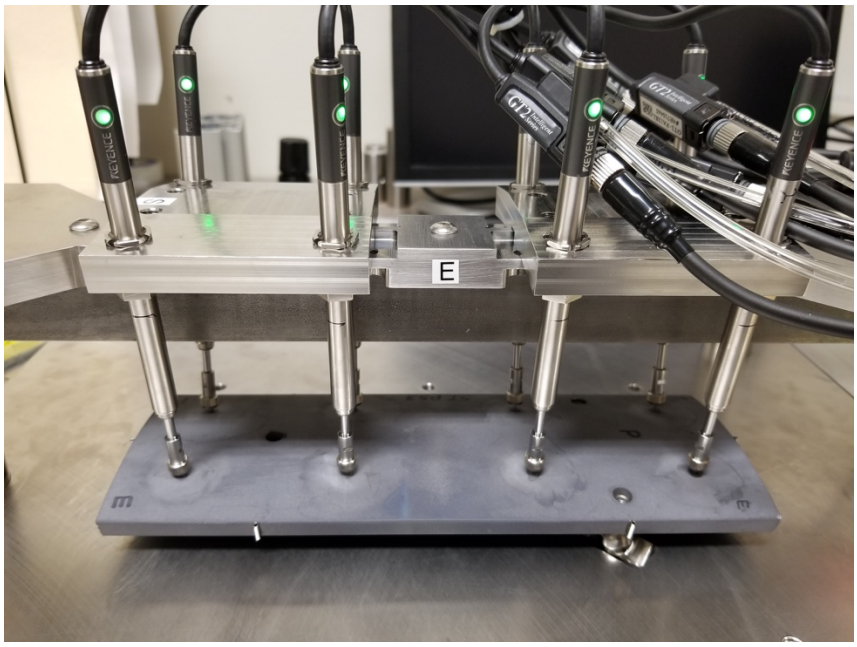

Figure 4. Spacer heights measuring probes. Eight probes are mounted on a stiff steel structure, with the probes positioned and inclined at the angles corresponding to those of the spacers (±7.5° from vertical). The probes are pressure-activated and contact the spacers at their tips. The underlying mirror mount is kinematically set using 3 steel balls. Each probe has a ready resolution of 0.1 μm and a short-term repeatability of < 0.2 μm (rms).

2.3 Spacer heights correction to produce perfect focusing

Once the centroids of the sub-apertured images are mapped, the focusing corrections for pitch and yaw are determined, from which the amount of spacer corrections is inferred. It is easy to see that the correction for pitch error involves spacer height removal of a pair of spacers at the same axial position, while that for the yaw error concerns the spacers in the diagonal. Typically, the amount of spacer height to be removed is ~ 1 μm, depending on how well the spacers were set to begin with.

Once the Hartmann centroid map is taken and the necessary amount for correction of spacer heights is determined, the mirror is removed from the mount and the mount is moved to the grinding station to be worked on. The radius gauges, again, are used to determine the change of spacer heights to within ≈ 0.1 – 0.2 μm. The Hartmann process is iterated to refine the alignment until accurate alignment is achieved. The process is relatively slow and we are working on improving its efficiency. In the near future, we plan to implement a setup such that the spacer material removal can be done in-situ.

For the grinding process, presently, we simply grind away the spacer materials with a set of specially made grinding tools. The tools consist of pads imbedded with diamond grits of various sizes, which are, in turn, attached to elastic pads. The elastic pads are needed to maintain the shape of the top surfaces of the spacers. The amount to be removed is simply controlled by timing the grinding. A picture of the setup is shown in Figure 5. The advantage of such method is that it is quite straightforward and simple to setup. The downside is that it is difficult to pre-calibrate the removal rates accurately. The removal rates depend on the loading of the polishing tools, the history and

condition of the grinding pads, and the surface condition of the spacers. Therefore, the actual removal rates have to be determined from the radius gauges and finer errors will come from iteration of the Hartmann measurements.

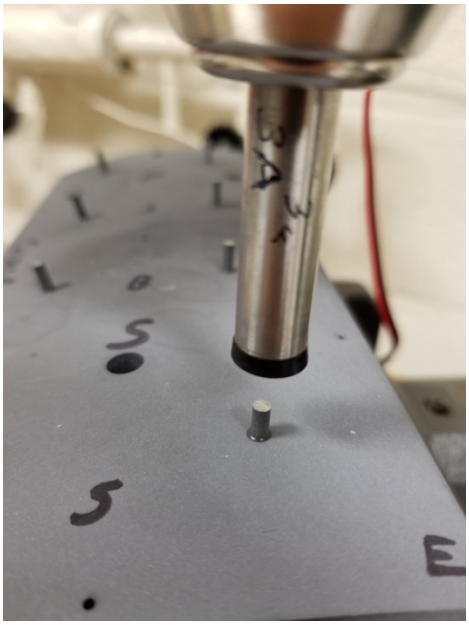

Figure 5. Spacer modification by polishing. Special grinding tools were prepared to effect spacer height reduction. The tools consist of pads imbedded with diamond grits of various sizes, which are, in turn, attached to elastic pads. The elastic pads are needed to maintain the shape of the top surfaces of the spacers. Successively finer grinding is necessary to bring the spacer heights down for the alignment errors to converge to zero. The removal rates range from a few μm/min to few 0.1 μm/min, depending on the loading for the grinding, the condition/history of the polishers, and the roughness of the surface of the spacers.

3. BONDING OF MIRROR

When the focusing is optimal, the mirror is then bonded onto the spacers with a small amount of adhesive. The mirror is removed for the application of epoxy and the same agitation methods (acoustic or mechanical vibrations) can be used to position the mirror properly. This procedure introduces no additional error as long as the adhesive does not introduce additional "heights" after the mirror is replaced. That is, we require that any adhesive at the mirror-spacer contact points has to be completely pushed away. Currently, we use epoxy as the adhesive and the loading on the mirror to squeeze the epoxy fluid away is simply the weight of the mirror. The accuracy of positioning the mirror in the presence of epoxy (that is, negligible bond line at the contacts) naturally depends on the amount and the viscosity of the epoxy, the shape of the spacer-top, and the weight of the mirror.

3.1 Viscosity of epoxy

A negligible bond line in the present case means < 0.1 μm. For the typical mass of our mirrors (between 10 – 20 g) and for spacers with typical parameters, the placement is relatively successful as measured by the Hartmann measurements. Error in terms of delta-HPD is generally < 0.5″. However, the "yield" is not 100%, meaning that when the procedure does not result in an acceptable bond, the bonding is undone before the epoxy is dry. In that sense, the upper limit of the delta-HPD is simply our cut-off for acceptable bonding. Part of the reason for the variation is that the process is largely manual. We are in the process of developing a more controlled, machine-assisted process for replacing the mirror more accurately after the epoxy is applied.

We find that typical epoxy with a viscosity of $< 10^4$ cP (10 Pa.s) works well with our spacers of 3 mm in diameter. An epoxy with lower viscosity generally works better to allow the mirror to sink better. For experimentation, we use a Devcon brand of epoxy which is sufficiently fluid and has a reasonably short curing time. We also dilute the epoxy with solvents (mostly acetone) to modify the viscosity as needed.

Clearly, the epoxy we use for experimentation is not flight-qualified. It does not have sufficiently high bonding strength and it does not meet low outgassing standards. More work will need to be done to test bonding with different epoxies. Preliminary studies using epoxy with higher viscosity have been less successful.

3.2 Shape and size of spacer top surface and amount of epoxy

The shape of the spacer's top determines the volume that the epoxy can escape to in order for the spacers to maintain a point contact to the mirror's surface. When that is done properly, the epoxy forms a ring around the contact with negligible epoxy there, as the mirror "sinks" onto the spacers. Smaller amount of epoxy helps, so does spacers of smaller diameters. Both of them reduce the fluid's resistance to the motion of the mirror during the bonding process. We are less successful using spacers with larger diameters or large radius of curvature on their top surfaces. More extensive tests have to be done along these lines to obtain more quantitative characterizations of the dependencies on these parameters. We are planning to experiment with spacers of different diameters. However, spacers with smaller diameters as small as 1 mm are difficult to work with and they do not provide sufficient strength due to the small bond area. This is still an area of active study.

3.3 Curing

Epoxy is cured in room temperature before they are further cured at elevated temperatures. We have shown that curing the epoxy in room temperature overnight provides sufficient strength for transportation of the bonded mirrors to the x-ray testing facility for testing. It has also been demonstrated that such initial curing result in negligible change in mirror alignment.

However, further curing either at room or elevated temperatures do distort the mirrors. Local distortions around the bonding points are observed, so is mirror misalignment. Such instability of mirror alignment (one to several weeks in room temperature) is unsatisfactory and distortion due to epoxy curing is currently an area of intense research. We have set up stand-alone bonding experiments to directly test the nature of distortion due to bonding. We also have tracked performance of bonded mirrors to understand temporal characteristics of the epoxies and are evaluating the effects from different kinds of epoxies.

3.4 Aligning and bonding subsequent mirrors

Aligning the second mirror in a pair is similar to that of aligning the first mirror. As discussed above, the relative position of the two mirrors are pre-determined by the initial setting of the spacer heights, and they are accurate to ~ 1μm, which is adequate. The angular alignment of the second mirror, because of the obscuration of any direct reflection, will be based on the focusing from the double reflection off both mirrors. The procedure is exactly the same.

Once the mirrors in the previous shell are integrated stably, new spacers can be installed on the back of them. The process therefore can be repeated as the mirror stack is built up. Since we can set the total radial distance (relative to the base) of the stack of mirrors from the first to the n^{th} shell, the errors of spacer heights for the n^{th} shell do not grow as it would by just using the distance from the $(n-1)^{th}$ shell to the n^{th} shell (which will grow as $\sqrt{n}$). This lack of stacking error is important to building larger modules with high resolution.

Currently, we are integrating mirrors from the "inside out" ---mirrors with small radii were integrated first, and subsequent mirrors are mounted on the back of previous ones. It is also possible, perhaps even beneficial, to build up the mirror module "outside in". In that case, spacers with appropriate lengths have to be pre-installed on the mirrors to be bonded first, as the crown surface of each spacer will have to be the side that engages the mirror surface below. The pre-installed spacers on the current mirror can be modified at the mirror's back in the same way. Benefits of the "outside-in" scheme includes a simpler Hartmann measurement (no need to avoid the spacer locations that obscure light) and lower risk in the modification of spacers since the mirror stack is not directly involved in that procedure, unlike that in the "inside-out" scheme. As the control of mirror thickness gets better, and mass production process of spacers with specified dimensions are matured, such an "outside-in" scheme will become more preferable. We are actively pursuing such a scheme in our next series of bonding.

4. RESULTS AND NEXT PLANS

4.1 Current Test status from alignment and bonding

In the past year, we continued to align and bond mirror pairs using the continuously refined procedures outlined above and using improved silicon mirrors fabricated at GSFC. We used mirrors that were first polished and their figures further refined with ion-beam figuring. They were not coated with x-ray reflective metal, however. We will use metal coated mirrors later for higher x-ray reflectivity. The bonded mirrors (single pairs) were transported to a local x-ray testing facility, a 600 m long beamline, for x-ray testing. A Ti target operated at 15 kV was typically used. A liquid-nitrogen cooled, 1K x 1K x-ray CCD with 13 μm pixels, was placed at the focal plane. (The focal distance is longer than the designed $f = 8400$ mm, due to the non-negligible beam divergence even at a source distance of 600 m.) Since we are primarily interested in imaging quality, the x-ray CCD camera was operated in the imaging mode where the mirror pairs were fully or partially illuminated and x-ray events were allowed to pile up in single long exposures.

A recent result is shown in Figure 6. The bonded pair demonstrated a resolution of 1.2″ (half-power diameter, HPD), which is an improvement from the 2.3″ results obtained a year ago. Sub-aperture images were also taken. The imaging qualities of the mirror pair at mid-azimuth sectors were very good. Most of them were actually < 1″. The left panel of Figure 6 shows the image of the middle sector having an HPD of 0.5″.

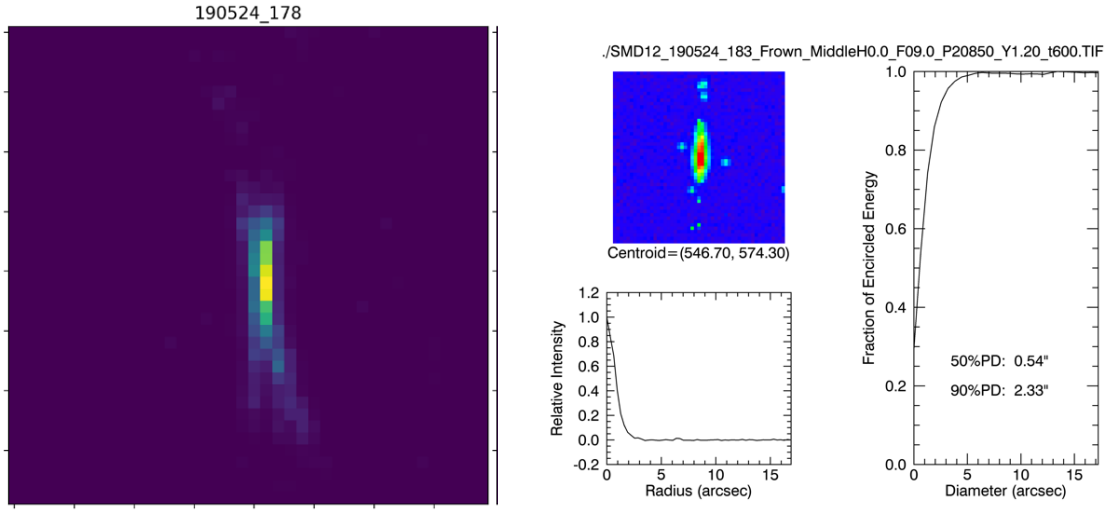

Figure 6. Result of a result x-ray test of a bonded pair of mirrors. (Left) Fully illuminated mirrors demonstrates a resolution of 1.2″ (HPD). (Right) A single sub-aperture window of 3° at mid-azimuth shows a sector HPD of 0.5″, confirming the excellent intrinsic axial figure of the mirrors.

Since the axial profile of the mirrors at the azimuthal middle is good (< 1″), the remaining errors are mostly concentrated at the two sides of the mirrors. The contributing factors are identified as alignment errors, bonding distortion, gravity distortion, and substrate imperfection at the sides. All these factors tend to be worse at the sides than at the azimuthal middle. It is likely that bonding distortion is the dominant error term. In fact, instability of images was observed in x-ray tests, indicating the importance of the role played by epoxy curing. In the test result shown above, HPD began to degrade within days and went beyond 2″ in a week (even though the degradation slowed down significantly in the next 4 weeks.) We will have more to report once their relative contributions are identified quantitatively.

4.2 Plans

To advance the alignment and bonding technology further, we plan to concentrate our efforts in the following three areas: (1) To improve the current alignment and bonding process of single pairs and better understand the systematic errors and uncertainties. The tasks include studies of systematic errors arising from optical metrology, bonding distortion, and instability. (2) To align and bond two or more pairs. We plan to integrate mirrors from multiple shells

into a small module, demonstrating precision in shell-to-shell alignment. (3) After successful x-ray tests, we plan to carry out environmental tests to elevate the technology readiness level.

For alignment, since the random error in the measurement is 0.3″, cases with larger alignment mismatch between optical and x-ray measurements indicate systematic issues. We are checking the parallelism of the optical beam over scales of approximately 5 cm in the azimuthal direction. The off-axis parabola, which generates the optical parallel beam, is being investigated. Interference fringes generated over aperture as small as 0.5 mm in the mirror's radial direction can also be an issue. Other systematic effects include imperfect reflection and interference effects in the optical path from the silicon mirrors to the camera, and stray light entering the camera. For bonding distortion and associated instability, we are investigating the types and amount of epoxy used.

To demonstrate the alignment of mirrors from shell to shell, we plan to build a module with more than one pair of mirrors. Since the alignment and bonding method is, in principle, independent of existing mirrors in the module, the main item to demonstrate is the precision of the image position on the focal plane, as well as metrology issues, such as interference, when other mirrors exist in the module. As discussed in Section 2, alignment error due to uncertainties arising from the translation of mirrors in the plane parallel to the focal plane is quite negligible. However, the shift of image position on the focal plane due to the "roll" of the mirrors can no longer be ignored. Spacers on one side of the mirrors will have to be made precisely, relative to the other side, in order to co-align the images from mirrors in different shells.

In parallel of these efforts, we are carrying out detailed finite-element modelling and stand-alone strength tests, to prepare for building a prototype that will undergo environmental tests such as vibration, acoustic, and thermal-vacuum tests, in order to ready the technology for future missions.

REFERENCES

[1] J. A. Gaskin, et al., "The Lynx X-ray Observatory: concept study overview and status," Proc. SPIE, 10699, 106990N (2018)
[2] S. L. O'Dell, et al., "High resolution x-ray optics," Proc. SPIE, 7803, 78030H (2010).
[3] W. Zhang, et al., "High-resolution, lightweight, and low-cost x-ray optics for the Lynx Observatory," J. Astro. Teles. Instr. Sys., 5(2), 021012 (2019).
[4] W. Zhang, et al., "Astronomical x-ray optics using monocrystalline silicon: high resolution, light weight, and low cost," Proc. SPIE, 10699, 106990O (2018).
[5] R. E. Riveros, et al., "Fabrication of lightweight silicon x-ray mirrors for high-resolution x-ray optics," Proc. SPIE, 10699, 106990P (2018).
[6] H. Mori, et al., "Reflective coatings for the future x-ray mirror substrates," Proc. SPIE, 10699, 1069941 (2018).
[7] Y. Yao, et al., "Thermal oxide patterning method for compensating coating stress in silicon x-ray telescope mirrors," Proc. SPIE, 10699, 1069942 (2018).
[8] B. D. Chalifoux, et al., "Compensating film stress in silicon substrates for the Lynx x-ray telescope mission concept using ion implantation," Proc. SPIE, 10699, 1069959 (2018).
[9] H. E. Zuo, et al., "Ultrafast laser micro-stressing for correction of thin fused silica optics for the Lynx x-ray telescope mission," Proc. SPIE, 10699, 1069954 (2018).
[10] K. W. Chan, et al., "Alignment and bonding of silicon mirrors for high-resolution astronomical x-ray optics," Proc. SPIE, 10699, 1039940 (2018).
[11] T. Saha, et al., "Optical design of the STAR-X telescope," Proc. SPIE, 10399, 10399 (2017).
[12] R. S. McClelland, et al., "The STAR-X x-ray telescope assembly (XTA)," Proc. SPIE, 10399, 10399 (2017).
[13] W. Zhang, et al., "Next generation astronomical x-ray optics: high-resolution, lightweight, and low-cost," Proc SPIE, 11119, 11119xx (2019)
[14] R. E. Riveros, et al., "Fabrication of mono-crystalline silicon mirrors for x-ray telescopes," Proc. SPIE, 11119, 11119xx (2019).
[15] Y. Yao, et al., "Development of a thermal-oxide patterning method for mitigating coating stress-induced distortion in silicon mirrors for the Lynx x-ray telescope mission concept," Proc. SPIE, 11119, 11119xx (2019).

[16] H. E. Zuo, et al., “Demonstration of ultrafast laser micro-stressing in correction of thin silicon optics for x-ray telescopes,” Proc. SPIE, 11119, 11119xx (2019).
[17] K. W. Chan, et al., “Recent advances in the alignment of silicon mirrors for high-resolution x-ray optics,” Proc. SPIE, 11119, 11119xx (2019).
[18] M. P. Biskach, et al., “Manufacturing of high-resolution and lightweight monocrystalline silicon x-ray optics at scale,” Proc. SPIE, 11119, 11119xx (2019).
[19] P. M. Solly, et al., “Structural analysis and testing of silicon x-ray mirror modules,” Proc. SPIE, 11119, 11119xx (2019).
[20] T. Saha, W. Zhang, “Design optimization for x-ray telescopes,” Proc. SPIE 11119, 11119xx (2019).